Effects of strangeness on the chiral pseudocritical line

Mahammad Sabir Ali,[1,*] Deeptak Biswas,[1,†] Amaresh Jaiswal,[1,2,‡] and Hiranmaya Mishra[1,§]

[1]*School of Physical Sciences, National Institute of Science Education and Research, An OCC of Homi Bhabha National Institute, Jatni-752050, India*

[2]*Institute of Theoretical Physics, Jagiellonian University, ul. St. Łojasiewicza 11, 30-348 Krakow, Poland*

(Received 25 March 2024; accepted 16 May 2024; published 12 June 2024)

Within a $2+1$ flavor Nambu–Jona-Lasinio model, we calculate the curvature coefficients and check them against available lattice QCD estimations. With the observation that the flavor mixing due to the 't Hooft determinant term significantly affects the κ_2^S, we explore the effect of μ_S on the $T-\mu_B$ crossover lines. With the novel determination of negative κ_2^B at large μ_S, we advocate the importance of studying the same in lattice QCD.

DOI: 10.1103/PhysRevD.109.114017

I. INTRODUCTION

The phase diagram of the strongly interacting matter necessitates the determination of the chiral transition line in the high-density and high-temperature regions. The chiral symmetry is broken in the low-density (-temperature) phase of quantum chromodynamics (QCD), which gets restored as the temperature and/or density increases. At vanishing baryon density, the restoration of the chiral symmetry is determined to be a crossover with a pseudocritical temperature $T_{\rm pc} = 156.5 \pm 1.5$ MeV [1]. On the other hand, the transition is expected to be a first order at high density, which is connected to the crossover line through a critical end point (CEP). Although the determination of the crossover line for small values of the baryon chemical potential (μ_B) is quite settled with the recent advancements of lattice QCD (LQCD) [1,2] calculations, the extension of the line at finite μ_B suffers from the infamous sign problem, which leads to the oscillatory behavior of the Monte Carlo sampling method.

For small chemical potential (μ_X), the pseudocritical line can be Taylor expanded at the lowest order in μ_X^2, where one defines the line with the following ansatz [1–3]:

$$\frac{T_{\rm pc}(\mu_X)}{T_{\rm pc}(0)} = 1 - \kappa_2^X \left(\frac{\mu_X}{T_{\rm pc}(0)}\right)^2 - \kappa_4^X \left(\frac{\mu_X}{T_{\rm pc}(0)}\right)^4. \quad (1)$$

Here, μ_X corresponds to chemical potential associated with various charges like baryon charge B, electric charge Q, and strangeness S. Such a parametrization allows for the comparison of results from different models and lattice QCD calculations within the same baseline. The curvature coefficients κ_2 and κ_4 have been examined by the Taylor expansion method on the lattice [1,4,5]. Another standard approach relies on performing the calculations at imaginary chemical potential, followed by an analytic continuation to the real plane [2,6,7]. The abovementioned results are in good agreement with each other within the respective variances. Similar studies have been performed within the perturbative QCD [8] as well as in the ideal and mean-field hadron resonance gas (HRG) model [9,10] and quark-meson model [11–16]. Moreover, the Nambu–Jona-Lasinio (NJL) model has also been employed in this context [17] considering two flavors of light quarks.

The effective models, considering the symmetries of the QCD Lagrangian, enable one to probe the matter at extreme conditions like high temperature and/or density, even in the presence of a magnetic field, to understand the phases of the QCD matter and provide a bulk description [18,19]. The NJL model relies on chiral symmetry and provides a qualitative description of the QCD matter considering the pseudoscalar mesons [20,21]. Despite the analytical simplicity and the dependence on the parameter sets of such an effective model, the estimations made with the NJL model are quite robust [22,23]. It acts as a suitable alternative for benchmark estimation at high-density and low-temperature regions [24], as there is no restriction on the applicability of this model at finite density.

Over the past few decades, LQCD and NJL have complemented each other while broadening our understanding of strong interaction in various scenarios. For example, magnetic catalysis (MC) was first shown within an NJL framework [25,26]. Two decades later, lattice QCD not only looked at the MC feature [27–31], but also observed inverse magnetic catalysis around the crossover temperature [31]. This results in better versions of NJL models with nonlocal interactions [32] and external agent-dependent interaction

*sabir@niser.ac.in
†deeptakb@niser.ac.in
‡a.jaiswal@niser.ac.in
§hiranmaya@niser.ac.in

strength [33,34]. Further, in an NJL-like model, the anomalous breaking of $U(1)_A$ symmetry is addressed by explicitly adding the 't Hooft determinant interaction (characterized by coupling G_d), which also represents the flavor mixing. Recently, Refs. [35,36] explored the effect of G_d on isospin-sensitive observables in a two-flavor NJL model and constrained G_d using the same from LQCD. In the context of the three-flavor NJL model, G_d is the most ill-constrained parameter with a large allowed range while reproducing acceptable values of physical observables [22,23].

In this paper, for the first time in the $2+1$ flavor case with isospin symmetry, the effect of the G_d is explored by incorporating a finite strangeness chemical potential. This provides an opportunity to study the effect of a large μ_S on the pseudocritical line and provide novel estimations. Although the large variation of μ_S (0–200) MeV is beyond the scope of the freeze-out lines in heavy-ion collisions owing to strangeness neutrality, the present investigation is of particular interest for extending the NJL model at very high density. We organized this paper as follows: In Sec. II, we describe the model formalism for a $2+1$ flavor NJL model with the isospin symmetry. We present our results in Sec. III and summarize our findings in Sec. IV.

II. FORMALISM

The $2+1$-flavor NJL model Lagrangian is given by

$$\mathcal{L}_{\rm NJL} = \bar{\psi}(i\gamma_\mu\partial^\mu - \hat{m})\psi + \mathcal{L}_{\rm S} + \mathcal{L}_{\rm D}, \tag{2}$$

where the four- and six-point interaction terms are given by

$$\begin{aligned}\mathcal{L}_{\rm S} &= G_s\sum_{a=0}^{8}\left[(\bar{\psi}\lambda_a\psi)^2 + (\bar{\psi}i\gamma_5\lambda_a\psi)^2\right],\\ \mathcal{L}_{\rm D} &= -G_d\left[\det\bar{\psi}_i(1-\gamma_5)\psi_j + \det\bar{\psi}_i(1+\gamma_5)\psi_j\right].\end{aligned} \tag{3}$$

Here, $\psi^{\rm T} = (u, d, s)$ is the quark triplet in flavor space with an up, down, and strange quark, and $\hat{m} = {\rm diag}(m_u, m_d, m_s)$ is the current quark mass matrix. In the interaction, the λ's are the Gell-Mann matrices, and in $\mathcal{L}_{\rm D}$, the determinant is taken in the flavor space. $\mathcal{L}_{\rm S}$ represents the four-quark interaction, with the coupling strength G_s, which is symmetric under $U(3)\times U(3)$ symmetry. On the other hand, $\mathcal{L}_{\rm D}$, with coupling strength G_d, describes the six-quark interactions known as the 't Hooft determinant. $\mathcal{L}_{\rm D}$ is included to break the $U(1)_A$ symmetry explicitly as $U(1)_A$ is anomalous in quantum theory.

To obtain the free energy, it is standard to introduce auxiliary fields using the Hubbard-Stratonovich transformation [37] to make the Lagrangian quadratic in fermion fields. Within mean-field approximation, we can have nonzero vacuum expectation values of these auxiliary fields. In the absence of any other external agents (like a magnetic field, isospin chemical potential, etc.), symmetry only allows the $\bar{\psi}\psi$ channel to acquire nonzero vacuum expectation values, and the mean-field Lagrangian becomes

$$\mathcal{L}_{\rm MFA} = \bar{\psi}(i\gamma_\mu\partial^\mu - \hat{M})\psi - 2G_s\sum_i\sigma_i^2 + 4G_d\prod_i\sigma_f, \tag{4}$$

where $\hat{M}$ is the constituent mass matrix, and the constituent masses are given by [22]

$$M_i = m_i - 4G_s\sigma_i + 2G_d\epsilon_{ijk}\sigma_j\sigma_k, \tag{5}$$

with $\sigma_i = \langle\bar{\psi}_i\psi_i\rangle$ being the condensate that works as the order parameter of chiral symmetry breaking. As it is evident from the above equation, G_d mixes different flavors.

It is straightforward to integrate out the fermion degrees of freedom from Eq. (4) to obtain the free energy. To introduce temperature (T) and chemical potentials (μ_f), it is customary to perform the following transformations [38]:

$$p_0 \to ip_4 - \mu_f, \qquad p_4 = (2n+1)\pi T. \tag{6}$$

With the above transformation, the integration over p_0 gets replaced by the sum over Mastubara frequencies, n. Moreover, the free energy is given by [39,40]

$$\Omega = \Omega_{\rm MF} + \Omega_{\rm Vac} + \Omega_{\rm Th}, \tag{7}$$

where

$$\Omega_{\rm MF} = 2G_s\sum_i\sigma_i^2 - 4G_d\prod_i\sigma_i, \tag{8}$$

$$\Omega_{\rm Vac} = -2N_c\sum_i\int^{\Lambda}\frac{d^3p}{(2\pi)^3}\varepsilon_i(p), \tag{9}$$

$$\begin{aligned}\Omega_{\rm Th} = -2N_cT\sum_i\int\frac{d^3p}{(2\pi)^3}\Big[&\ln\left(1+e^{-(\varepsilon_i(p)-\mu_i)/T}\right)\\ &+\ln\left(1+e^{-(\varepsilon_i(p)+\mu_i)/T}\right)\Big].\end{aligned} \tag{10}$$

With $N_c = 3$ the number of colors, $\varepsilon_i(p) = \sqrt{\vec{p}^2 + M_i^2}$ is the energy of the ith flavor quark, and Λ is the three-momentum cutoff.

To obtain the ground state, one can minimize the free energy defined in Eq. (7) by solving the following gap equations simultaneously:

$$\frac{\partial\Omega}{\partial\sigma_u} = \frac{\partial\Omega}{\partial\sigma_d} = \frac{\partial\Omega}{\partial\sigma_s} = 0. \tag{11}$$

In this study, we have considered the isospin symmetric case; in other words, the electric charge and associated chemical potential (μ_Q) are ignored, which implies that $\sigma_u = \sigma_d = \sigma_l$. The quark chemical potential can be written in terms of baryon and strangeness chemical potential

TABLE I. Parameter sets of the NJL model used in the present work. Set I and II are from Hatsuda and Kunihiro [22] and Rehberg *et al.* [23], respectively.

	Λ (MeV)	$G_s\Lambda^2$	$G_d\Lambda^5$	m_l (MeV)	m_s (MeV)
Set I	631.4	1.835	9.29	5.5	135.7
Set II	602.3	1.835	12.36	5.5	140.7

$$\mu_u = \mu_d = \frac{1}{3}\mu_B,$$
$$\mu_s = \frac{1}{3}\mu_B - \mu_S. \tag{12}$$

Finally, for a fixed μ_B and μ_S, we define the pseudocritical temperature ($T_{\rm pc}$) as the inflection temperature where the curvature of σ_l changes sign [15]. In the context of LQCD, $T_{\rm pc}$ is generally determined from the maximum of the chiral susceptibility [15].

Let us note that there are five parameters in this three-flavor NJL model, namely, the current quark mass for the strange and light quarks (m_s and m_l), two coupling G_s and G_d, and the three-momentum cutoff Λ. After choosing the $m_l = 5.5$ MeV, consistent with chiral perturbation theory [41], the remaining four parameters are fixed by fitting the pion decay constant and the masses of the pion, kaon, and η' [22,23] to their empirical values. We have considered two widely used parameter sets from Refs. [22,23] given in Table I. With the parametrization of set I, the mass of the η meson is underestimated by 11%, while for set II, the same is underestimated by 6%. As seen from Table I, the dimensionless coupling $G_d\Lambda^5$ differs by 30% between the two sets, translating into a 70% variation in G_d. In this work, we intend to prescribe a way to constrain it more precisely.

III. RESULTS

We next consider the thermodynamics of this system to discuss chiral phase transition using Eqs. (7)–(12). For a given value μ_B and μ_S, the pseudocritical temperature ($T_{\rm pc}$) is defined to be the inflection point of light quark condensate (the order parameter of chiral symmetry breaking) as a function of the temperature. Before proceeding to investigate the effect of finite μ_S on the $T-\mu_B$ line, it is essential to check the model estimation against the available lattice QCD results of the curvature coefficients ($\kappa_{2,4}$). Considering $\mu_Q = 0$, we have first investigated the $T-\mu_B$ ($\mu_S = 0$) and $T-\mu_S$ ($\mu_B = 0$) plane, and find the $\kappa_{2,4}$ by parametrizing the respective pseudocritical lines with the ansatz of Eq. (1) for the range $\mu_{B,S}/T_{\rm pc}(0) \le 1.0$ with $T_{\rm pc}(0) = 171.1$ and 173.4 MeV for parameter sets I and II, respectively.

We have tabulated our estimations for the curvature coefficients κ_2 and κ_4 in Tables II and III, respectively.

TABLE II. Estimations of κ_2 for the two parameter sets. The lattice QCD results are taken from Refs. [1,7].

	κ_2^B ($\mu_S = 0$)	κ_2^S ($\mu_B = 0$)	$\kappa_2^{B,n_S=0}$
NJL, set I	0.01627	0.01345	0.01478
NJL, set II	0.01619	0.01719	0.01350
Lattice QCD	0.016(6) [1]	0.017(5) [1]	0.012(4) [1]
			0.0153(18) [7]

TABLE III. Values of κ_4 for the pseudocritical line for different cases.

	κ_4^B ($\mu_S = 0$)	κ_4^S ($\mu_B = 0$)	$\kappa_4^{B,n_S=0}$
NJL, set I	0.00006	0.001477	0.000081
NJL, set II	0.00005	0.001892	0.000742
Lattice QCD	0.001(7) [1]	0.004(6) [1]	0.000(4) [1]
			0.00032(67) [7]

The lattice results are taken from the HotQCD Collaboration [1] and WB Collaboration [2]. There is excellent agreement with LQCD estimations for κ_2 in both the $T-\mu_B$ and $T-\mu_S$ line. We would like to emphasize that the values of κ_2^B are similar for both the parameter sets, which infers that the large difference in G_d between two parameter sets does not influence the $T-\mu_B$ phase line. On the contrary, for the $\mu_B = 0$ plane, κ_2^S is distinctly different for the two parameter sets. Although these κ_2^S values match the lattice estimations within the variances, the estimation with parameter set II has a better agreement with the mean value. The difference in the κ_2^S is attributed to G_d, which brings the influence of a strange quark to the light quarks as pointed out in Eq. (5). This motivates us to examine the effect of G_d on κ_2^B by exploring the $T-\mu_B$ line at various values of μ_S.

To appreciate the effects arising from the strange sector, we have restricted this study to smaller values of baryon chemical potential [up to $\mu_B/T_c(0) \le 1.0$] and varied the μ_S from 0 to 200 MeV. We have restricted the μ_S within half the kaon mass to exclude the possibility of kaon condensation [42]. Because of the difference in the magnitude of the $T_{\rm pc}$ between the NJL and lattice studies, we have scaled the results with their respective $T_{\rm pc}(\mu_B = 0)$ as shown in Fig. 1. As may be observed, for finite values of μ_S, the $T_{\rm pc}$ initially increases with μ_B and then decreases. For smaller values of μ_B, a finite μ_S decreases the thermal weight in the strange sector [μ_S comes with a negative sign in the strange thermal distribution; see Eq. (12)] and therefore leads to a higher value of $T_{\rm pc}/T_{\rm pc}(0)$ for the same μ_B as shown in Fig. 1. As μ_B increases further, this rise in $T_{\rm pc}$ gets saturated and eventually starts decreasing.

For the first time, such a prominent increase in the pseudocritical temperature ($T_{\rm pc}$) along the $T-\mu_B$ line is

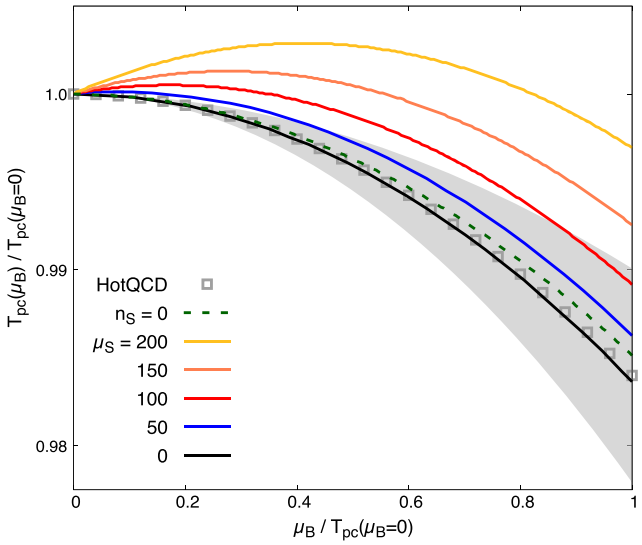

FIG. 1. Phase line in the $T-\mu_B$ plane for different μ_S, evaluated with parameter set I. For representative purposes, axes are scaled with respective $T_{\rm pc}(\mu_B=0)$. The continuous lines represent our estimations for various values of μ_S. The data and band are from the HotQCD Collaboration [1]. The dashed line corresponds to the strangeness neutral case.

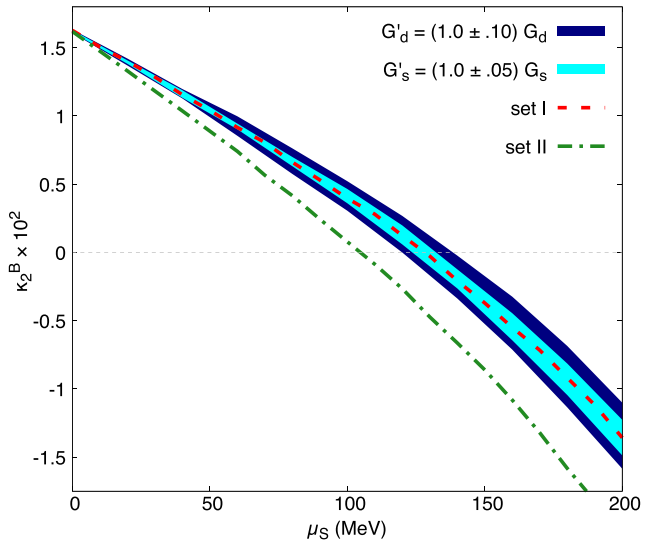

FIG. 2. κ_2^B as a function of μ_S in MeV. The red (dashed) and green (dashed-dot) lines are the central values for sets I and II, respectively. The blue and cyan bands are associated with a $\pm 10\%$ change in G_d and a $\pm 5\%$ change in G_s, respectively, for parameter set I.

observed, which arises due to a finite strangeness chemical potential. This trend was not observed in earlier studies within LQCD [1,43] and HRG [10], as most of them were performed along the $\mu_S = 0$ line or along the freeze-out line, where the strangeness neutrality sets up the limit of $\mu_S \leq \mu_B/3$ [43].

To quantify the increase in the $T_{\rm pc}$ with μ_B for a given value of μ_S, we have used the ansatz of Eq. (1) to extract the curvature coefficients. We have presented the variation of κ_2^B with μ_S in Fig. 2 for both the parameter sets. The curvature coefficient κ_2^B starts from a positive value for $\mu_S = 0$ and decreases as we increase the strangeness chemical potential. We wish to emphasize that with μ_S, κ_2^B decreases from its positive value at $\mu_S = 0$ and eventually becomes negative at some $\mu_S = \mu_S^c$. This negative sign of κ_2^B is one of the novel results of the present investigation. This was not observed earlier in the context of the pseudocritical line [1,7]. One important observation is that the μ_S^c are distinctively different for the two parameter sets. $G_s\Lambda^2$ being the same for both the sets, this difference in μ_S^c is essentially due to the variance in G_d. A large G_d provides a stronger influence of the strange quark sector on the light quarks, resulting in a faster decrease in κ_2^B.

At this juncture, it is instructive to check κ_2^B along the strangeness neutrality line ($n_S = 0$). A finite μ_B requires the strangeness chemical potential $\mu_S \neq 0$ to achieve zero net strangeness. This corresponds to $\mu_S = \mu_B/3$ as we are considering $\mu_Q = 0$, and there is no vector interaction in the present model. We have found $\kappa_2^{B,n_S=0} < \kappa_2^{B,\mu_S=0}$ as listed in Table II. The decrease of κ_2^B for the strangeness neutral case is commensurate with the lattice estimations [1,43] and in accordance with our findings of the reduction of κ_2^B with μ_S. We would like to comment here that the behavior of the κ_2^B ($\mu_S \neq 0$) is similar to the lattice QCD calculations. The lattice estimations of $n_S = 0$ correspond to values of μ_S, which are not large enough to constrain the flavor mixing determinant coupling. This necessitates LQCD simulations at a larger value of μ_S.

It would be interesting to check the robustness of this negative κ_2^B on the parametrization of the NJL model itself. For this purpose, we have varied G_s, G_d by 5% and 10%, respectively, and examined the effect on the κ_2^B variation as shown in Fig. 2. As discussed earlier, a larger value for G_d increases the coupling between the light and strange sector resulting in a faster decrease of κ_2^B. Needless to say, κ_2^B becomes independent of μ_S at $G_d = 0$ as the strange and light quark sector decouple, which is evident in the Lagrangian of the NJL model. On the contrary, the variation of G_s has a weaker effect on the features mentioned above.

Within LQCD, the numerical value of κ_4^B is consistent with zero [1,7], as for the small value of $\mu_{B,S}/T$, the fourth order coefficients of the μ_X/T expansion are prone to having a weaker effect on the $T-\mu_X$ line. In the present study, we have found κ_4 to have good agreement for the case ($\mu_B \neq 0, \mu_S = 0$) and ($\mu_B = 0, \mu_S \neq 0$) as shown in Table III. It would be essential to investigate the same for the $T-\mu_B$ line at various μ_S. For larger values of μ_S, we have found the κ_4 to be finite (as in Fig. 3), even with the different parameter sets, as mentioned earlier. These findings suggest that even within the small μ_B range, a nonzero κ_4 is possible by switching on a finite strangeness chemical

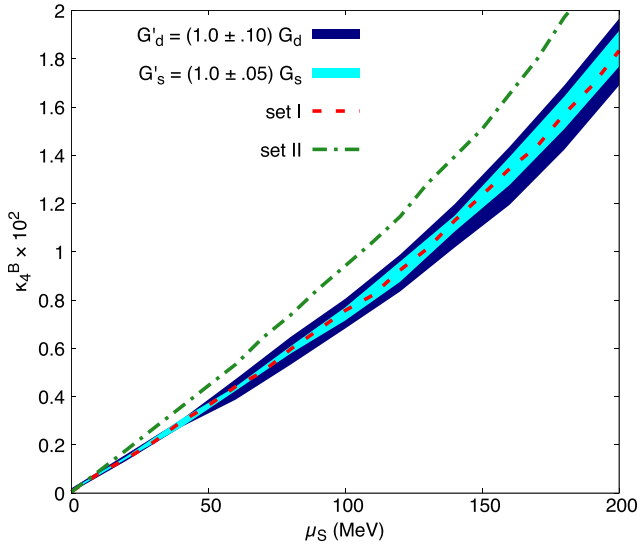

FIG. 3. κ_4^B as a function of μ_S in MeV. Color code is the same as Fig. 2.

potential μ_S, which is relevant in the context of lattice simulations.

IV. SUMMARY AND CONCLUSION

In this paper, we have explored the chiral phase boundary of the QCD matter within a $2+1$ flavor Nambu–Jona-Lasinio model with special emphasis on the effect of strangeness on the curvature coefficients κ_2^B and κ_4^B. To our knowledge, this is the first such exploration within a $2+1$ NJL model. We have considered the isospin symmetric case and $\mu_Q = 0$. To have better control over the lowest-order coefficients (κ_2^X), we have limited the study within the range $\mu_X/T \leq 1$. As a benchmark, we have first estimated the $\kappa_{2,4}^X$ for three separate cases: (1) the $T-\mu_B$ plane ($\mu_S = 0$) i.e., $\kappa_{2,4}^B$, (2) the $T-\mu_S$ plane ($\mu_B = 0$), i.e., $\kappa_{2,4}^S$, and (3) along the strangeness neutrality line $\kappa_{2,4}^{B,n_S=0}$. We have used two standard sets of parametrizations of the $2+1$ NJL model that differ significantly regarding the flavor mixing determinant interaction. Although we have an excellent agreement of κ_2^B with the available LQCD finding for both parameter sets, we have observed that κ_2^S has a strong dependence on the flavor mixing and $U(1)_A$ breaking 't Hooft interaction. Between the two parameter sets used, set II with a higher value of G_d reproduces the lattice estimation of κ_2^S better. To explore the effects of flavor mixing through G_d, it is instructive to study the μ_S dependence of the $T-\mu_B$ lines, which have been quantified by estimating κ_2^B as a function of μ_S.

It is interesting to note that, we have observed for the first time the decreasing behavior of κ_2^B with μ_S, which is interesting, and interpreting it in the framework of the NJL model is also relevant. More importantly, we have found that it becomes negative for sufficiently large values of μ_S. Further, it is also observed that the value of μ_S where κ_2^B vanishes is different for the two parameter sets. This difference is attributed to the fact that a larger value of G_d strengthens the strange contribution to the light sector, resulting in a faster decrease. We expect that the outcomes from LQCD investigations for κ_2^B at large enough μ_S will assist in better constraining the 't Hooft coupling G_d, thereby enhancing our understanding of effective models like NJL and the underlying QCD. In this article, we have prescribed a way to quantify the flavor mixing, which is an important development toward understanding the effective model and, eventually, QCD.

At this juncture, we note that the physical scenarios accessible in the present heavy-ion collision experiments are rather constrained to $n_S = 0$ and $n_Q = 0.4n_B$. However, from a theoretical perspective, it is possible to explore QCD in all directions as it helps one to calibrate and understand various aspects of the theory. Lattice QCD has explored the phase diagram at finite μ_Q and μ_S [1], and recently, it has been extended toward a larger value of strangeness chemical potential [43]. Our study provides an alternate approach in this direction. We have investigated here the low μ_B region of the phase diagram for the study of curvature coefficients. The effect of flavor mixing on CEP in the presence of finite μ_S will be interesting and deserves a separate investigation which will be explored in a future work.

ACKNOWLEDGMENTS

D. B. is supported in part by the Department of Science and Technology, Government of INDIA under the SERB National Post-Doctoral Fellowship Reference No. PDF/2023/001762. M. S. A. and D. B. would like to extend thanks to C. A. Islam for the fruitful discussions and critical reading of the manuscript.

[1] A. Bazavov *et al.* (HotQCD Collaboration), Chiral crossover in QCD at zero and non-zero chemical potentials, Phys. Lett. B **795**, 15 (2019).

[2] R. Bellwied, S. Borsanyi, Z. Fodor, J. Günther, S. D. Katz, C. Ratti, and K. K. Szabo, The QCD phase diagram from analytic continuation, Phys. Lett. B **751**, 559 (2015).

[3] C. Bonati, M. D'Elia, F. Negro, F. Sanfilippo, and K. Zambello, Curvature of the pseudocritical line in QCD: Taylor expansion matches analytic continuation, Phys. Rev. D **98**, 054510 (2018).

[4] R. V. Gavai and S. Gupta, Pressure and nonlinear susceptibilities in QCD at finite chemical potentials, Phys. Rev. D **68**, 034506 (2003).

[5] R. V. Gavai and S. Gupta, The critical end point of QCD, Phys. Rev. D **71**, 114014 (2005).

[6] C. Bonati, M. D'Elia, M. Mariti, M. Mesiti, F. Negro, and F. Sanfilippo, Curvature of the chiral pseudocritical line in QCD: Continuum extrapolated results, Phys. Rev. D **92**, 054503 (2015).

[7] S. Borsanyi, Z. Fodor, J. N. Guenther, R. Kara, S. D. Katz, P. Parotto, A. Pasztor, C. Ratti, and K. K. Szabo, QCD crossover at finite chemical potential from lattice simulations, Phys. Rev. Lett. **125**, 052001 (2020).

[8] N. Haque and M. Strickland, Next-to-next-to leading-order hard-thermal-loop perturbation-theory predictions for the curvature of the QCD phase transition line, Phys. Rev. C **103**, 031901 (2021).

[9] D. Biswas, P. Petreczky, and S. Sharma, Chiral condensate from a hadron resonance gas model, Phys. Rev. C **106**, 045203 (2022).

[10] D. Biswas, P. Petreczky, and S. Sharma, Chiral condensate and the equation of state at non-zero baryon density from hadron resonance gas model with repulsive mean-field, Phys. Rev. C **109**, 055206 (2024).

[11] W.-j. Fu, J. M. Pawlowski, and F. Rennecke, QCD phase structure at finite temperature and density, Phys. Rev. D **101**, 054032 (2020).

[12] B.-J. Schaefer and J. Wambach, The phase diagram of the quark meson model, Nucl. Phys. **A757**, 479 (2005).

[13] J. Braun, B. Klein, and B.-J. Schaefer, On the phase structure of QCD in a finite volume, Phys. Lett. B **713**, 216 (2012).

[14] C. S. Fischer and J. Luecker, Propagators and phase structure of $N_f = 2$ and $N_f = 2 + 1$ QCD, Phys. Lett. B **718**, 1036 (2013).

[15] J. M. Pawlowski and F. Rennecke, Higher order quark-mesonic scattering processes and the phase structure of QCD, Phys. Rev. D **90**, 076002 (2014).

[16] C. S. Fischer, J. Luecker, and C. A. Welzbacher, Phase structure of three and four flavor QCD, Phys. Rev. D **90**, 034022 (2014).

[17] M. Buballa, NJL model analysis of quark matter at large density, Phys. Rep. **407**, 205 (2005).

[18] S. K. Ghosh, T. K. Mukherjee, M. G. Mustafa, and R. Ray, Susceptibilities and speed of sound from PNJL model, Phys. Rev. D **73**, 114007 (2006).

[19] R. C. Pereira, Quantum chromodynamics phase diagram under extreme conditions, Ph.D. thesis, Coimbra University, 2021, https://hdl.handle.net/10316/95294.

[20] Y. Nambu and G. Jona-Lasinio, Dynamical model of elementary particles based on an analogy with superconductivity. 1, Phys. Rev. **122**, 345 (1961).

[21] Y. Nambu and G. Jona-Lasinio, Dynamical model of elementary particles based on an analogy with superconductivity. II, Phys. Rev. **124**, 246 (1961).

[22] T. Hatsuda and T. Kunihiro, QCD phenomenology based on a chiral effective Lagrangian, Phys. Rep. **247**, 221 (1994).

[23] P. Rehberg, S. P. Klevansky, and J. Hufner, Hadronization in the SU(3) Nambu-Jona-Lasinio model, Phys. Rev. C **53**, 410 (1996).

[24] A. Mishra and H. Mishra, Chiral symmetry breaking, color superconductivity and color neutral quark matter: A variational approach, Phys. Rev. D **69**, 014014 (2004).

[25] S. P. Klevansky and R. H. Lemmer, Chiral symmetry restoration in the Nambu-Jona-Lasinio model with a constant electromagnetic field, Phys. Rev. D **39**, 3478 (1989).

[26] V. P. Gusynin, V. A. Miransky, and I. A. Shovkovy, Catalysis of dynamical flavor symmetry breaking by a magnetic field in $(2 + 1)$-dimensions, Phys. Rev. Lett. **73**, 3499 (1994); **76**, 1005(E) (1996).

[27] P. V. Buividovich, M. N. Chernodub, E. V. Luschevskaya, and M. I. Polikarpov, Numerical study of chiral symmetry breaking in non-Abelian gauge theory with background magnetic field, Phys. Lett. B **682**, 484 (2010).

[28] P. V. Buividovich, M. N. Chernodub, E. V. Luschevskaya, and M. I. Polikarpov, Chiral magnetization of non-Abelian vacuum: A lattice study, Nucl. Phys. **B826**, 313 (2010).

[29] V. V. Braguta, P. V. Buividovich, T. Kalaydzhyan, S. V. Kuznetsov, and M. I. Polikarpov, The chiral magnetic effect and chiral symmetry breaking in SU(3) quenched lattice gauge theory, Phys. At. Nucl. **75**, 488 (2012).

[30] M. D'Elia and F. Negro, Chiral properties of strong interactions in a magnetic background, Phys. Rev. D **83**, 114028 (2011).

[31] G. S. Bali, F. Bruckmann, G. Endrodi, Z. Fodor, S. D. Katz, and A. Schafer, QCD quark condensate in external magnetic fields, Phys. Rev. D **86**, 071502 (2012).

[32] V. P. Pagura, D. Gomez Dumm, S. Noguera, and N. N. Scoccola, Magnetic catalysis and inverse magnetic catalysis in nonlocal chiral quark models, Phys. Rev. D **95**, 034013 (2017).

[33] R. L. S. Farias, K. P. Gomes, G. I. Krein, and M. B. Pinto, Importance of asymptotic freedom for the pseudocritical temperature in magnetized quark matter, Phys. Rev. C **90**, 025203 (2014).

[34] M. Ferreira, P. Costa, O. Lourenço, T. Frederico, and C. Providência, Inverse magnetic catalysis in the $(2 + 1)$-flavor Nambu-Jona-Lasinio and Polyakov-Nambu-Jona-Lasinio models, Phys. Rev. D **89**, 116011 (2014).

[35] M. S. Ali, C. A. Islam, and R. Sharma, Studying explicit U(1)A symmetry breaking in a hot and magnetized two flavor nonlocal NJL model constrained using lattice results, Phys. Rev. D **104**, 114026 (2021).

[36] M. S. Ali, C. A. Islam, and R. Sharma, The role of $U(1)_A$ symmetry breaking in the QCD corrections to the pion mass difference, J. Phys. G **50**, 115003 (2023).

[37] J. Hubbard, Calculation of partition functions, Phys. Rev. Lett. **3**, 77 (1959).

[38] M. G. Mustafa, An introduction to thermal field theory and some of its application, Eur. Phys. J. Special Topics **232**, 1369 (2023).

[39] F. Gastineau, R. Nebauer, and J. Aichelin, Thermodynamics of the three flavor NJL model: Chiral symmetry breaking and color superconductivity, Phys. Rev. C **65**, 045204 (2002).

[40] H. Kohyama, D. Kimura, and T. Inagaki, Regularization dependence on phase diagram in Nambu–Jona-Lasinio model, Nucl. Phys. **B896**, 682 (2015).

[41] J. Gasser and H. Leutwyler, Quark masses, Phys. Rep. **87**, 77 (1982).

[42] A. Barducci, R. Casalbuoni, G. Pettini, and L. Ravagli, Pion and kaon condensation in a 3-flavor NJL model, Phys. Rev. D **71**, 016011 (2005).

[43] H. T. Ding, O. Kaczmarek, F. Karsch, P. Petreczky, M. Sarkar, C. Schmidt, and S. Sharma, Curvature of the chiral phase transition line from the magnetic equation of state of $(2 + 1)$-flavor QCD, arXiv:2403.09390.